

# Photon Energy Spectrum in $B \rightarrow X_s + \gamma$ and comparison with Data

A. Ali

Deutsches Elektronen Synchrotron DESY, Hamburg, Germany

C. Greub<sup>1</sup>

SLAC Theory Division, Stanford University, USA

## Abstract

A comparison of the inclusive photon energy spectrum in the radiative decay  $B \rightarrow X_s + \gamma$ , measured recently by the CLEO collaboration, with the standard model is presented, using a  $B$ -meson wave function model and improving earlier perturbative QCD-based computations of the same. The dependence of the photon energy spectrum on the non-perturbative model parameters,  $p_F$ , the  $b$ -quark Fermi momentum in the  $B$  hadron, and  $m_q$ , the spectator quark mass, is explicitly shown, allowing a comparison of these parameters with the ones obtained from the analysis of the lepton energy spectrum in semileptonic  $B$  decays. Taking into account present uncertainties, we estimate  $\text{BR}(B \rightarrow X_s + \gamma) = (2.55 \pm 1.28) \times 10^{-4}$  in the standard model, assuming  $|V_{ts}|/|V_{cb}| = 1.0$ . Comparing this with the CLEO measurement  $\text{BR}(B \rightarrow X_s + \gamma) = (2.32 \pm 0.67) \times 10^{-4}$  implies  $|V_{ts}|/|V_{cb}| = 1.1 \pm 0.43$ , in agreement with the CKM unitarity.

---

<sup>1</sup> Supported by Schweizerischer Nationalfonds.

# 1 Introduction

Recently, the CLEO collaboration has reported the first measurement of the photon energy spectrum in the decay  $B \rightarrow X_s + \gamma$  [1], following the measurement of the exclusive decay mode  $B \rightarrow K^* + \gamma$  reported in 1993 by the same collaboration [2]. The inclusive branching ratio and the photon energy spectrum allow a less model-dependent comparison with the underlying theory, more specifically the standard model (SM), as compared to the exclusive decay modes which require additionally decay form factors. The CLEO data have been compared in [1] with the SM-based theoretical computations presented in [3] - [5], allowing to draw the conclusion that agreement between theoretical predictions and experiment is good, given that large uncertainties exist in both. In particular, the measured branching ratio  $\text{BR}(B \rightarrow X_s + \gamma) = (2.32 \pm 0.67) \times 10^{-4}$  [1] is in agreement with the SM-based estimates in [3, 5], as well as with the ones in [6, 7].

In this letter, we would like to report on an improved calculation of the photon energy spectrum compared to what we have presented earlier and which has been used in the CLEO analysis [1]. The main theoretical difference lies in the inclusion of the complete operator basis  $O_1, \dots, O_8$  for the effective Hamiltonian, defined below, in the computation of the partonic processes  $b \rightarrow s + \gamma$  and  $b \rightarrow s + g + \gamma$ , and in using the complete leading-logarithmic computations of the anomalous dimension matrix presented in [8]. In contrast, our previous calculations were done in the truncated approximation, where we had dropped the effects of the four-Fermi operators  $O_3, \dots, O_6$  and the chromomagnetic operator  $O_8$  in the computation of the contributions from  $b \rightarrow s + g + \gamma$ . In addition, use was made of the anomalous dimension matrix derived in [9]. The other ingredient of our calculation, namely a specific  $B$ -meson wave function model [10, 11] to incorporate the non-perturbative effects on spectra, remains unaltered. However, since data are now available, we fit the normalized photon energy spectrum with the improved theoretical framework to determine from the shape the non-perturbative parameters of the wave function model being used, namely the Fermi motion parameter  $p_F$  and the spectator quark mass  $m_q$ . These in turn determine within the model the  $b$ -quark mass. There is considerable theoretical interest in these parameters, in particular  $p_F$ , which is a good measure of the kinetic energy of the  $b$  quark in the  $B$  meson, and the  $b$ -quark mass. Since a similar framework has also been used, in conjunction with the perturbative QCD-improved parton model, in the analysis of the lepton energy spectrum in inclusive  $B$ -meson decays [1], it is interesting to compare the model parameters obtained from the two measurements. While, admittedly, present errors are large preventing us from drawing sharp conclusions, some valuable insight on the shape parameters and normalization can already be obtained and we quantify this information.

This letter is organized as follows: In section 2, we briefly summarize the effective Hamiltonian for the decay  $B \rightarrow X_s + \gamma$  and present the Wilson coefficients numerically. Section 3 contains an anatomy of the partonic processes  $b \rightarrow s + \gamma$  and  $b \rightarrow s + g + \gamma$ , where the essential steps in the derivation of the matrix elements are given. The photon energy spectrum at the partonic level is derived in section 4, including a discussion of the Sudakov behaviour in the end-point region. Section 5 summarizes the  $B$ -meson wave function model [10, 11]. Numerical results for the branching ratio  $\text{BR}(B \rightarrow X_s + \gamma)$  in the SM, the ratio of the Cabibbo-Kobayashi-Maskawa (CKM) matrix elements  $|V_{ts}|/|V_{cb}|$ , and fits of the CLEO photon energy spectrum from  $B \rightarrow X_s + \gamma$  with our theoretical estimates, yielding a  $\pm 1\sigma$ -contour in the parameter space  $(p_F, m_q)$  are given in section 6.

## 2 Effective Hamiltonian for the decay $B \rightarrow X_s + \gamma$

The framework we use here is that of an effective theory with five quarks, obtained by integrating out the heavier degrees of freedom, which in the standard model are the top quark and the  $W$ -boson. A complete set of dimension-6 operators relevant for the processes  $b \rightarrow s + \gamma$  and  $b \rightarrow s + \gamma + g$  is contained in the effective Hamiltonian

$$H_{eff}(b \rightarrow s\gamma) = -\frac{4G_F}{\sqrt{2}} \lambda_t \sum_{j=1}^8 C_j(\mu) O_j(\mu) \quad , \quad (1)$$

where  $G_F$  is the Fermi constant coupling constant and  $C_j(\mu)$  are the Wilson coefficients evaluated at the scale  $\mu$ , and  $\lambda_t = V_{tb}V_{ts}^*$  with  $V_{ij}$  being the CKM matrix elements. The operators  $O_j$  read

$$\begin{aligned} O_1 &= (\bar{c}_{L\beta} \gamma^\mu b_{L\alpha}) (\bar{s}_{L\alpha} \gamma_\mu c_{L\beta}) \quad , \\ O_2 &= (\bar{c}_{L\alpha} \gamma^\mu b_{L\alpha}) (\bar{s}_{L\beta} \gamma_\mu c_{L\beta}) \quad , \\ O_3 &= (\bar{s}_{L\alpha} \gamma^\mu b_{L\alpha}) \left[ (\bar{u}_{L\beta} \gamma_\mu u_{L\beta}) + \dots + (\bar{b}_{L\beta} \gamma_\mu b_{L\beta}) \right] \quad , \\ O_4 &= (\bar{s}_{L\alpha} \gamma^\mu b_{L\beta}) \left[ (\bar{u}_{L\beta} \gamma_\mu u_{L\alpha}) + \dots + (\bar{b}_{L\beta} \gamma_\mu b_{L\alpha}) \right] \quad , \\ O_5 &= (\bar{s}_{L\alpha} \gamma^\mu b_{L\alpha}) \left[ (\bar{u}_{R\beta} \gamma_\mu u_{R\beta}) + \dots + (\bar{b}_{R\beta} \gamma_\mu b_{R\beta}) \right] \quad , \\ O_6 &= (\bar{s}_{L\alpha} \gamma^\mu b_{L\beta}) \left[ (\bar{u}_{R\beta} \gamma_\mu u_{R\alpha}) + \dots + (\bar{b}_{R\beta} \gamma_\mu b_{R\alpha}) \right] \quad , \\ O_7 &= (e/16\pi^2) \bar{s}_\alpha \sigma^{\mu\nu} (m_b(\mu)R + m_s(\mu)L) b_\alpha F_{\mu\nu} \quad , \\ O_8 &= (g_s/16\pi^2) \bar{s}_\alpha \sigma^{\mu\nu} (m_b(\mu)R + m_s(\mu)L) (\lambda_{\alpha\beta}^A/2) b_\beta G_{\mu\nu}^A \quad , \end{aligned} \quad (2)$$

where  $e$  and  $g_s$  are the electromagnetic and the strong coupling constants, respectively. In the magnetic moment type operators  $O_7$  and  $O_8$ ,  $F_{\mu\nu}$  and  $G_{\mu\nu}^A$  denote the electromagnetic and the gluonic field strength tensors, respectively.  $L = (1 - \gamma_5)/2$  and  $R = (1 + \gamma_5)/2$  denote the left and right-handed projection operators. We note here that the explicit mass factors in  $O_7$  and  $O_8$  are the running quark masses. QCD corrections to the decay rate for  $b \rightarrow s\gamma$  bring in large logarithms of the form  $\alpha_s^n(m_W) \log^m(m_b/M)$ , where  $M = m_t$  or  $m_W$  and  $m \leq n$  (with  $n = 0, 1, 2, \dots$ ). To get a reasonable result, one should resum at least the leading logarithmic contribution (i.e.  $m = n$ ) to all orders. Using the renormalization group equation the Wilson coefficient can be calculated at the scale  $\mu \approx m_b$  which is the relevant scale for  $B$  decays. At this scale the large logarithms are contained in the Wilson coefficients. As we are working in this paper to leading logarithmic precision, it is sufficient to know the leading order anomalous dimension matrix and the matching  $C_i(\mu = m_W)$  to lowest order (i.e., without QCD corrections) [12]. The  $8 \times 8$  matrix is given in <sup>2</sup> [8] and the Wilson coefficients are explicitly listed in [6, 13]. The numerical values of the Wilson coefficients that we use in our calculations are given in table 1. For subsequent discussion we define two effective Wilson coefficients  $C_7^{eff}(\mu)$  and  $C_8^{eff}(\mu)$  below and give their numerical values in table 1:

$$\begin{aligned} C_7^{eff} &\equiv C_7 + Q_d C_5 + 3Q_d C_6 \quad , \\ C_8^{eff} &\equiv C_8 + C_5 \quad . \end{aligned} \quad (3)$$

---

<sup>2</sup>The results given here for the entries concerning  $O_7$  and  $O_8$  correspond to the naive dimensional regularization scheme (NDR), which we use in the calculation of all the matrix elements.

$C_i(\mu)$	$\mu = m_W$	$\mu = 10.0 \text{ GeV}$	$\mu = 5.0 \text{ GeV}$	$\mu = 2.5 \text{ GeV}$
$C_1$	0.0	-0.158	-0.235	-0.338
$C_2$	1.0	1.063	1.100	1.156
$C_3$	0.0	0.007	0.011	0.016
$C_4$	0.0	-0.017	-0.024	-0.034
$C_5$	0.0	0.005	0.007	0.009
$C_6$	0.0	-0.019	-0.029	-0.044
$C_7$	-0.193	-0.290	-0.333	-0.388
$C_8$	-0.096	-0.138	-0.153	-0.171
$C_7^{eff}$	-0.193	-0.273	-0.306	-0.347
$C_8^{eff}$	-0.096	-0.132	-0.146	-0.162

Table 1: Wilson coefficients  $C_i(\mu)$  at the scale  $\mu = m_W = 80.33 \text{ GeV}$  (“matching conditions”) and at three other scales,  $\mu = 10.0 \text{ GeV}$ ,  $\mu = 5.0 \text{ GeV}$  and  $\mu = 2.5 \text{ GeV}$ , evaluated with two-loop  $\beta$ -function and the leading-order anomalous-dimension matrix. The entries correspond to the top quark mass  $\overline{m}_t(m_t^{pole}) = 170 \text{ GeV}$  (equivalently,  $m_t^{pole} = 180 \text{ GeV}$ ) and the QCD parameter with 5 flavours  $\Lambda_5 = 195 \text{ MeV}$  (equivalently,  $\alpha_s(m_Z^2) = 0.117$ ), both in the  $\overline{MS}$  scheme.

### 3 An anatomy of the processes $b \rightarrow s\gamma$ and $b \rightarrow s\gamma g$

We summarize the principal points of the derivation of the photon energy spectrum in the decay  $b \rightarrow s\gamma(+g)$  in this letter and refer to [14] for technical details. As it is the process  $b \rightarrow s\gamma g$  which leads to a nontrivial photon energy spectrum at the partonic level, we strive at taking it fully into account. The amplitude for this decay suffers from infrared singularities as the gluon or the photon energy goes to zero. The topology of the decay  $b \rightarrow s\gamma g$  resembles that of the two-body decays  $b \rightarrow s\gamma$  and  $b \rightarrow sg$  in the limit as  $E_g \rightarrow 0$  or  $E_\gamma \rightarrow 0$ , respectively. The singular configurations in  $b \rightarrow s\gamma g$  are cancelled in a distribution sense in the photon energy spectrum if one also takes into account virtual corrections to the two-body process  $b \rightarrow sg$  and  $b \rightarrow s\gamma$ , order by order in perturbation theory. We will take into account only those virtual correction diagrams which are needed to cancel the infrared singularities from  $b \rightarrow s\gamma g$ .

We first discuss the result for  $b \rightarrow s\gamma$ . It turns out that the effects of the four-Fermi operators to  $b \rightarrow s\gamma$  can be absorbed into a redefinition of the coefficient  $C_7 \rightarrow C_7^{eff}$ , with  $C_7^{eff}$  defined in eq. (3). This not only holds for the  $b \rightarrow s\gamma$  amplitude without virtual corrections but also for those infrared-sensitive virtual corrections which we have mentioned above. One therefore has to calculate the matrix element of  $C_7^{eff} O_7$  for  $b \rightarrow s\gamma$  including virtual corrections. The result of this calculation, which was derived in  $d = 4 - 2\epsilon$  dimensions, can be expressed as [3]:

$$\Gamma_7^{virt} = \Gamma_{7,sing}^{virt} + \Gamma_{7,fin}^{virt}, \quad (4)$$

where we have split this quantity into an infrared-finite and an infrared-singular part:

$$\Gamma_{7,sing}^{virt} = -\frac{m_b^5}{96\pi^5} (1-r)^3 (1+r) |C_7^{eff} G_F \lambda_t|^2 \alpha_{em} \alpha_s \frac{\left(\frac{4\pi\mu^2}{m_b^2}\right)^{2\epsilon}}{\Gamma(2-2\epsilon)} \left[ \frac{4}{\epsilon} + \frac{2(1+r)}{1-r} \frac{\log r}{\epsilon} \right], \quad (5)$$

and

$$\Gamma_{7,fin}^{virt} = \frac{m_b^5}{32\pi^4} (1-r)^3 (1+r) |C_7^{eff} G_F \lambda_t|^2 \alpha_{em} (1 + \frac{\alpha_s}{3\pi} \tau), \quad (6)$$

$$\tau = \left\{ \left( \frac{1+r}{1-r} \right) (\log^2 r - 4 \log r + 4 \log r \log(1-r)) - 8 + 3 \log r + 8 \log(1-r) - 2 \log \frac{\mu^2}{m_b^2} \right\}. \quad (7)$$

The quantity  $r$  is defined as  $r = (m_s/m_b)^2$ . The infrared singularity (5) will be cancelled when taking into account the gluon bremsstrahlung diagrams involving the operator  $O_7$ .

As we already noted, the process  $b \rightarrow s\gamma g$  has also an infrared singularity as the photon becomes soft. These singularities are cancelled analogously by virtual photon corrections to the matrix element for  $b \rightarrow sg$ , i.e. in  $C_8^{eff} O_8$ . The result is

$$\Gamma_8^{virt} = \Gamma_{8,sing}^{virt} + \Gamma_{8,fin}^{virt}, \quad (8)$$

$$\Gamma_{8,sing}^{virt} = -\frac{m_b^5}{96\pi^5} (1-r)^3 (1+r) |Q_d C_8^{eff} G_F \lambda_t|^2 \alpha_{em} \alpha_s \frac{\left( \frac{4\pi\mu^2}{m_b^2} \right)^{2\epsilon}}{\Gamma(2-2\epsilon)} \left[ \frac{4}{\epsilon} + \frac{2(1+r)}{1-r} \frac{\log r}{\epsilon} \right] \quad (9)$$

$$\Gamma_{8,fin}^{virt} = \frac{m_b^5}{96\pi^5} (1-r)^3 (1+r) |Q_d C_8^{eff} G_F \lambda_t|^2 \alpha_{em} \alpha_s \tau, \quad (10)$$

where  $\tau$  is given in eq. (7) and  $Q_d = -1/3$ . A remark concerning the quark masses is in order here. When calculating the matrix elements we have used the on-shell subtraction prescription for the quark masses. Due to the explicit factors of the running quark masses in the operators  $O_7$  and  $O_8$ , the  $m_b^5$  factor contained in  $\Gamma_7^{virt}$  and  $\Gamma_8^{virt}$  given above should be replaced by the following product

$$m_b^5 \longrightarrow m_{b,pole}^3 m_b(\mu)^2, \quad (11)$$

where  $m_{b,pole}$  and  $m_b(\mu)$  denote the pole mass and the running mass of the  $b$  quark, respectively. In actual practice, we identify all the masses  $m_b$  in the various intermediate expressions with  $m_{b,pole}$  and multiply at the end the so-derived decay width  $\Gamma(B \rightarrow X_s + \gamma)$  with a correction factor  $R$ :

$$R = (m_b(\mu)/m_{b,pole})^2, \quad (12)$$

as also advocated in [6].

We now take up the matrix elements for the process  $b \rightarrow s\gamma g$ . As the explicit expressions are too long to be presented here, we only point out the basic structure and give the complete formulae elsewhere [14]. We first concentrate on the contributions of the four-Fermi operators  $O_1, \dots, O_6$ . It turns out that the diagrams which do not involve both gauge particle radiation from an internal quark are either zero or can be absorbed into a redefinition of the coefficients  $(C_7, C_8) \rightarrow (C_7^{eff}, C_8^{eff})$ . The remaining case, in which both gauge particles are emitted from the internal fermion line, is discussed now. There are two such diagrams associated with each four-Fermi operator, whose sum is ultraviolet (and infrared) finite. We denote these matrix elements by  $M_i$

$$M_i = \frac{4G_F}{\sqrt{2}} \langle s\gamma g | C_i O_i | b \rangle, \quad (i = 1, 2, \dots, 6) \quad (13)$$

Analogously, the matrix elements of  $C_7^{eff} O_7$  and  $C_8^{eff} O_8$  are denoted by  $M_7$  and  $M_8$ , respectively. Adding all these contributions, the complete matrix element for  $b \rightarrow s\gamma g$  is denoted by

M

$$M = \sum_i^8 M_i \quad . \quad (14)$$

When squaring  $M$  and summing over the polarizations and spins of the particles, it turns out that only  $|M_7|_\Sigma^2$  and  $|M_8|_\Sigma^2$  are infrared-singular. The other squared amplitudes and all the interference terms are infrared-safe. We therefore make the decomposition

$$|M|_\Sigma^2 = F + |M_7|_\Sigma^2 + |M_8|_\Sigma^2 \quad , \quad (15)$$

where  $F$  denotes the infrared-safe contributions.

## 4 The photon energy spectrum at the partonic level

In the following, it is useful to define the dimensionless photon energy  $x$  through the relation

$$E_\gamma = \frac{m_b^2 - m_s^2}{2m_b} x \quad ;$$

$x$  then varies in the interval  $[0, 1]$ . The contribution of the  $F$ -term in eq. (15) to the spectrum  $d\Gamma_F/dx$  is completely finite and is worked out numerically. As the contribution  $d\Gamma_7^{brems}/dx$  associated with  $|M_7|_\Sigma^2$  is singular, we work it out analytically in  $d = 4 - 2\varepsilon$  dimensional phase space. Making use of the abbreviations  $r = (m_s/m_b)^2$  and  $\xi = (1-r)x$  the quantity  $d\Gamma_7^{brems}/dx$  can be written as

$$\begin{aligned} \frac{d\Gamma_7^{brems}}{dx} = & C_\varepsilon (1-r)^{-4\varepsilon} \frac{x^{-2\varepsilon}}{(1-x)^{1+2\varepsilon}} I_\varepsilon(x) + C_{\varepsilon=0} \left\{ \frac{x(2x^2 - 5x - 1)(1-r)}{1-\xi} \right. \\ & \left. + \frac{(1-r)x(1-x)(2x-1)}{(1-\xi)^2} - 2(1+x) \log(1-\xi) - I_{\varepsilon=0}(x) \right\} \quad , \quad (16) \end{aligned}$$

with

$$\begin{aligned} C_\varepsilon &= m_b^5 \frac{\left(\frac{4\pi\mu^2}{m_b^2}\right)^{2\varepsilon}}{\Gamma(2-2\varepsilon)} \frac{|G_F \lambda_t C_7^{eff}|^2}{96\pi^5} \alpha_{em} \alpha_s (1+r)(1-r)^3, \\ I_\varepsilon(x) &= I_a(x) + I_b(x)\varepsilon, \\ I_a &= -4 - \frac{4r}{1-\xi} - \frac{4}{\xi}(1+r) \log(1-\xi), \\ I_b &= \frac{8(1-\xi)}{\xi} \log(1-\xi) - \frac{4r}{1-\xi} \log(1-\xi) - \frac{8r}{1-\xi} + 8(1+r) \frac{\text{Li}(\xi)}{\xi} - \frac{2(1+r)}{\xi} \log^2(1-\xi). \end{aligned} \quad (17)$$

Here the symbol Li stands for the Spence function. The photon energy spectrum away from the endpoint  $x = 1$  can be obtained by taking the limit  $\varepsilon \rightarrow 0$  in eqs. (16) and (17). However, as the experimentally interesting region is just near this endpoint one has to add the virtual QCD corrections to the two-body process  $b \rightarrow s\gamma$ , as already mentioned. Before we discuss this further, we give the result for  $d\Gamma_8^{brems}/dx$ .

As  $d\Gamma_8^{brems}/dx$  has a non-integrable singularity at  $x = 0$  (i.e.,  $E_\gamma = 0$ ), we should work in  $d$ -dimensions as well. However, as the photon energy spectrum is of no experimental interest

at very small energies, i.e.  $E_\gamma \rightarrow 0$ , we remove the infrared regularization immediately. As for the branching ratio, we note that the dimensionally regularized total integral  $\Gamma_8^{brens}$  can be obtained from the analogous expression for  $\Gamma_7^{brens}$  by doing obvious replacements. The result for  $d\Gamma_8^{brens}/dx$  reads

$$\begin{aligned} \frac{d\Gamma_8^{brens}}{dx} = & m_b^5 \frac{|G_F \lambda_t Q_d C_8^{eff}|^2}{96\pi^5} \alpha_{em} \alpha_s (1+r)(1-r)^3 (1-x) \\ & \times \left\{ \frac{2[(1-r)x(x-2) + 2(1+r)]}{x(1-x)(1-r)} \log \frac{1-\xi}{r} + \right. \\ & \left. \frac{(1-r)(1-x)(1-2x)}{(1-\xi)^2} - \frac{(1-r)(2x^2 - x + 1)}{1-\xi} - \frac{8}{x} \right\} . \end{aligned} \quad (18)$$

Returning to the discussion of the infrared singularity of the quantity  $d\Gamma_7^{brens}/dx$  in eq. (16), which occurs for  $x \rightarrow 1$ , i.e., in the experimentally interesting region, we recall that this singularity is cancelled in a distribution sense if one takes into account the virtual QCD corrections to the tree level matrix element of  $O_7$  for the two-body process  $b \rightarrow s\gamma$ , given in eqs. (5) and (6). Technically, it is useful to define the integrated quantity

$$\Gamma_7(s_0) = \int_{s_0}^1 \left[ \frac{d\Gamma_7^{brens}}{dx} + \Gamma_7^{virt} \delta(1-x) \right] dx , \quad (19)$$

in which the singularities cancel manifestly. The expressions for  $d\Gamma_7^{brens}/dx$  and  $\Gamma_7^{virt}$  are given in eqs. (16) and (4), respectively. The explicit expression for  $\Gamma_7(s_0)$  reads

$$\Gamma_7(s_0) = V \left( 1 + \frac{\alpha_s}{3\pi} \Omega \right) \Theta(1-s_0) , \quad (20)$$

where  $\Theta$  is the step function and  $V$  is

$$V = m_b^5 \frac{|G_F \lambda_t C_7^{eff}|^2}{32\pi^4} \alpha_{em} (1+r)(1-r)^3 . \quad (21)$$

The expressions for  $\Omega$  is identical with the one that we had derived and presented earlier [4]. The difference lies in the normalization factor  $V$  given above. We have now included the complete operator basis,  $O_1, \dots, O_8$ , as opposed to our earlier calculations [3, 4] where use was made of a truncated basis neglecting the four-Fermi operators  $O_3, \dots, O_6$ . The difference reflects itself in the coefficient  $C_7$  used in [3, 4], which is now replaced by  $C_7^{eff}$ . The effective coefficient  $C_7^{eff}$  calculated with the anomalous dimension matrix given above is typically 10% smaller than  $C_7$  used by us earlier. From the definition of the quantity  $\Gamma_7(s_0)$  it is clear that the photon energy spectrum is reconstructed by differentiation, i.e.,

$$\frac{d\Gamma_7(x)}{dx}(x) = - \frac{d\Gamma_7(s_0)}{ds_0} \Big|_{s_0=x} . \quad (22)$$

The end-point spectra, however, show sensitivity to the leftover effects of the (cancelled) infrared singularity, with the photon-energy distribution rising very steeply near the end-point,  $x \simeq 1$ . Furthermore, there is still a  $\delta$ -function contribution sitting at  $x = 1$ , stemming from differentiation of the  $\Theta$  function in eq. (20). To remedy this, one often resorts to (an all order) resummation of the leading (infrared) logarithms. This resummation is done at the level of the quantity  $\Gamma_7(s_0)$ , i.e., before one derives the spectrum by the differentiation just described.

Although we are using for  $\Omega$  the expression for a non-zero strange quark mass (i.e.  $r \neq 0$ ) in the numerics [4], it is nevertheless instructive to look at the limit  $r \rightarrow 0$ . Splitting  $\Omega$  into two parts  $\Omega = \Omega_1 + \Omega_2$  and using the notation  $s_1 = (1 - s_0)$  we get

$$\begin{aligned}\Omega_1 &= -2 \log^2 s_1 - 7 \log s_1, \\ \Omega_2 &= -2 \log \frac{\mu^2}{m_b^2} - \frac{4\pi^2}{3} - 5 + 10s_1 + s_1^2 - \frac{2}{3}s_1^3 + s_1(s_1 - 4) \log s_1.\end{aligned}\quad (23)$$

Before giving the exponentiated analogue of eq. (20), we point out that the lepton energy spectrum in the inclusive semileptonic decays  $b \rightarrow u(+g)\ell\nu_\ell$ , in the limit of neglecting the final-state quark mass, has a similar structure [15, 16]. The leading term, i.e. the Sudakov double-log [17] in eq. (23), also enters in the lepton energy spectrum in the mentioned semileptonic decays with the same coefficient. However, as shown here and earlier [3, 4] (and also discussed in [18]), the coefficients of the non-leading logarithmic and power terms in the inclusive decay  $B \rightarrow X_s + \gamma$  and the semileptonic decay  $B \rightarrow X_u\ell\nu_\ell$  are different<sup>3</sup>. Therefore, the photon energy spectrum in  $B \rightarrow X_s + \gamma$  at the parton level can not be gotten from the lepton energy spectrum in the decays  $B \rightarrow X_u\ell\nu_\ell$ . For a recent discussion of the Sudakov-improved photon energy spectrum in  $B \rightarrow X_s + \gamma$ , see [19]. Finally, the exponentiated analogue of  $\Gamma_7(s_0)$  in eq. (20) reads

$$\Gamma_7^{exp}(s_0) = V \left(1 + \frac{\alpha_s}{3\pi} \Omega_2\right) \exp\left(\frac{\alpha_s}{3\pi} \Omega_1\right) \Theta(1 - s_0) \quad . \quad (24)$$

The explicit expressions for  $\Omega_1$  and  $\Omega_2$  for  $r \neq 0$  are given in [4]. The expression for the photon energy spectrum can again be obtained by differentiation:

$$\frac{d\Gamma_7^{exp}(x)}{dx}(x) = -\frac{d\Gamma_7^{exp}(s_0)}{ds_0}\bigg|_{s_0=x} \quad . \quad (25)$$

As exponentiation is required only near the end-point  $x \rightarrow 1$ , we use the exponentiated form in the region  $x > x_{crit}$  only. For numerical calculations we take  $x_{crit} = 0.85$ , where the transition from one form to the other works smoothly.

To summarize, the final answer for the photon energy spectrum for the process  $b \rightarrow s\gamma(+g)$ , where the  $b$  quark decays at rest, is given by

$$\frac{d\Gamma}{dx} = \frac{d\Gamma_F}{dx} + \Theta(x_{crit} - x) \frac{d\Gamma_7^{brems}}{dx} + \Theta(x - x_{crit}) \frac{d\Gamma_7^{exp}}{dx} + \frac{d\Gamma_8^{brems}}{dx} \quad , \quad (26)$$

where  $d\Gamma_F/dx$  is too long to be given here and is relegated to [14];  $d\Gamma_7^{brems}/dx$ ,  $d\Gamma_7^{exp}/dx$  and  $d\Gamma_8^{brems}/dx$  are given in eqs. (16), (25) and (18), respectively. A remark is in order here: As it stands, eq. (26) has still a singularity at the experimentally uninteresting point  $E_\gamma = 0$ , which is cancelled in a distribution sense when taking into account the virtual photon correction (see eq. (8)) of the operator  $O_8$ . In principle, one could do a resummation of the soft photons, in analogy with the treatment of the resummation of soft gluons just discussed above. As it turns out numerically, the contribution of photon energies below 50 MeV to the branching ratio is less than 1%, we just make a cut there and do not resort to any resummation in the  $E_\gamma \rightarrow 0$  limit.

---

<sup>3</sup>The discrepancy in the analytic results for the non-leading terms in [15] and [16] for the semileptonic decay seems to have been settled in favour of [16].

## 5 $B$ -meson Wave function Effects in $B \rightarrow X_s + \gamma$

In order to implement the  $B$ -meson bound state effects on the photon energy spectrum, we continue to use the wave-function model [10, 11] that we have used in our earlier work [4, 5]. We recall that this model has also been used in calculating the lepton energy spectra in inclusive  $D$ - and  $B$ -semileptonic decays. Assuming that the  $B$ -meson wave function effects are universal, the parameters of this model can be fixed from the semileptonic analysis and one can make a parameter-free comparison of the photon energy spectrum in  $B \rightarrow X_s + \gamma$  with data. This is what has been done in the experimental analysis of the data [1]. However, in general, the non-perturbative effects are likely to depend on the final-state quark mass, which, for example, is the case in the decays  $B \rightarrow X_s + \gamma$  and  $B \rightarrow X_c \ell \nu_\ell$ . It is, therefore, an interesting question to ask if the non-perturbative model being used by us consistently describes the lepton and photon energy spectra in the inclusive decays  $B \rightarrow X \ell \nu_\ell$  and  $B \rightarrow X_s \gamma$ , respectively. To answer this question quantitatively, one has to implement the perturbative QCD effects, as discussed in the previous section, incorporate the model, and confront the resulting framework with data to determine the model parameters with a well-defined statistical significance. This is what we shall undertake in this paper. We note that this point has also been investigated recently with a somewhat different non-perturbative (model) and perturbative(QCD) input in [19]. Due to detailed differences in the underlying theoretical frameworks and in the analysis of data, no direct quantitative comparison with this work is attempted here.

In the present model, which we refer to as the Fermi motion model, the  $B$ -meson consists of a  $b$ -quark and a spectator  $q$  and the four-momenta of the constituents are required to add up to the four-momentum of the  $B$ -meson. In the rest frame of the  $B$ -meson the  $b$ -quark and the spectator fly back-to-back with three momenta  $\vec{p}_b = -\vec{p}_q \equiv \vec{p}$ . Energy conservation then implies the equation

$$m_B = \sqrt{m_b^2 + \vec{p}^2} + \sqrt{m_q^2 + \vec{p}^2} \quad ,$$

which can only hold for all values of  $|\vec{p}|$ , if at least one of the masses becomes momentum dependent. In this model the spectator quark  $m_q$  is chosen to be a fixed, i.e. momentum-independent, parameter and the  $b$ -quark mass becomes momentum dependent. This momentum dependent  $b$ -quark mass is denoted by  $W$  in the following and is given by

$$W^2(p) = M_B^2 + m_q^2 - 2M_B \sqrt{p^2 + m_q^2} \quad . \quad (27)$$

The  $b$ -quark, whose decays determine the dynamics, is given a non-zero momentum having a Gaussian distribution, with the width determined by the parameter  $p_F$ :

$$\phi(p) = \frac{4}{\sqrt{\pi} p_F^3} \exp\left(\frac{-p^2}{p_F^2}\right) \quad ; \quad p = |\vec{p}| \quad (28)$$

We note that this wave function is normalized such that

$$\int_0^\infty dp p^2 \phi(p) = 1 \quad .$$

The photon energy spectrum from the decay of the  $B$ -meson at rest is then given by

$$\frac{d\Gamma}{dE_\gamma} = \int_0^{p_{max}} dp p^2 \phi(p) \frac{d\Gamma_b}{dE_\gamma}(W, p, E_\gamma) \quad , \quad (29)$$

where  $p_{max}$  is the maximally allowed value of  $p$  and  $\frac{d\Gamma_b}{dE_\gamma}$  is the photon energy spectrum from the decay of the  $b$ -quark in flight, having a mass  $W(p)$  and momentum  $p$ . This can be obtained by Lorentz boosting the  $b$ -quark decay spectrum at rest, which has been obtained in eq. (26).

## 6 Estimates of $\text{BR}(B \rightarrow X_s + \gamma)$ in the SM and the Parameters $(p_F, m_q)$

It is theoretically preferable to calculate the branching ratio for the inclusive decay  $B \rightarrow X_s + \gamma$  in terms of the semileptonic decay branching ratio

$$\text{BR}(B \rightarrow X_s \gamma) = \left[ \frac{\Gamma(B \rightarrow \gamma + X_s)}{\Gamma_{sl}} \right]^{th} \text{BR}(B \rightarrow X \ell \nu_\ell) \quad , \quad (30)$$

where, in the approximation of including the leading-order QCD correction,  $\Gamma_{sl}$  is given by the expression

$$\Gamma_{sl} = \frac{G_F^2 |V_{cb}|^2}{192\pi^3} m_b^5 g(m_c/m_b) (1 - 2/3 \frac{\alpha_s}{\pi} f(m_c/m_b)) \quad . \quad (31)$$

The phase space function  $g(z)$  is defined as

$$g(z) = 1 - 8z^2 + 8z^6 - z^8 - 24z^4 \ln(z) \quad , \quad (32)$$

and the function  $f(z)$  can be seen, for example, in ref. [10]. An approximate analytic form for  $f(z)$  has been obtained in [15]:

$$f(z) = (\pi^2 - \frac{31}{4})(1 - z)^2 + \frac{3}{2} \quad . \quad (33)$$

To get the branching ratio in eq. (30) we can proceed in two ways. One can either take the partonic (purely perturbative) expressions for both  $\Gamma(B \rightarrow X_s \gamma)$  and  $\Gamma_{sl}$  or one can first implement the wave function effects and then integrate the spectra. In the latter case, the dominant wave function effects in the quantity  $\Gamma_{sl}$  are included if one identifies  $m_b$  in eq. (31) with the effective value  $W_{eff}$  of the  $b$  quark mass, which is the value of the floating  $b$ -quark mass averaged over the Gaussian distribution:

$$W_{eff}^5 = \int dp p^2 \phi(p) W^5(p) \quad , \quad (34)$$

where  $W(p)$  is given in eq. (27). We remark that these procedures yield an almost identical branching ratio (within 1%), which shows that the Gaussian-distributed Fermi motion model [10, 11] is in agreement with the result that power corrections to the inclusive decay widths  $\Gamma(B \rightarrow X_s + \gamma)$  and  $\Gamma(B \rightarrow X \ell \nu_\ell)$ , calculated in the context of the heavy quark effective theory [20], cancel out in their ratio.

We now estimate  $\text{BR}(B \rightarrow X_s + \gamma)$  in the standard model and theoretical uncertainties on this quantity. The parameters that we have used in estimating the inclusive rates for  $\text{BR}(B \rightarrow X_s + \gamma)$  are summarized in table 2. The largest theoretical uncertainty stems from the scale dependence of the Wilson coefficients as was already stressed in [21]. The extent of this variation is somewhat correlated with the value of the QCD scale parameter  $\Lambda_5$  and the top quark mass. As given explicitly in the preceding section, the decay rate for  $B \rightarrow X_s + \gamma$  depends on seven of the eight Wilson coefficients given earlier, once one takes into account the bremsstrahlung corrections and is not factored in terms of a single (effective) coefficient, that one encounters for the two-body decays  $b \rightarrow s + \gamma$  [6]. To get some insight in the errors we enumerate here the values of the two dominant effective coefficients,  $C_7^{eff}$  and  $C_8^{eff}$ , as one varies  $\mu$ ,  $\Lambda_5$  and  $m_t$  in the range given in table 2:

$$\begin{aligned} C_7^{eff} &= -0.306 \pm 0.050 \\ C_8^{eff} &= -0.146 \pm 0.020 \end{aligned} \quad (35)$$

Parameter	Range
$\overline{m}_t$ (GeV)	$170 \pm 11$
$\mu$ (GeV)	$5.0^{+5.0}_{-2.5}$
$\Lambda_5$ (GeV)	$0.195^{+0.065}_{-0.05}$
$\mathcal{B}(B \rightarrow X \ell \nu_\ell)$	$(10.4 \pm 0.4)\%$
$m_c/m_b$	$0.29 \pm 0.02$
$m_W$ (GeV)	80.33
$\alpha_{\text{QED}}^{-1}$	130.0

Table 2: Values of the parameters used in estimating the branching ratio  $\text{BR}(B \rightarrow X_s + \gamma)$  in the standard model. The range of  $\Lambda_5$  is taken from the present world average (corresponding to  $\alpha_s(m_Z^2) = 0.117 \pm 0.005$ , using the two-loop  $\beta$ -function [22]) and the semileptonic branching ratio from [23].

The present theoretical uncertainties on these coefficients represent the dominant contribution to the theoretical error on  $\text{BR}(B \rightarrow X_s + \gamma)$ , contributing about  $\pm 35\%$ . The second source of scale-dependence is due to the appearance of the running quark masses in the operators  $O_7$  and  $O_8$ . As discussed in section 3, this brings into fore the extra (scale-dependent) multiplicative factor  $R = (m_b(\mu)/m_{b,pole})^2$  for the branching ratio  $\text{BR}(B \rightarrow X_s + \gamma)$ . The next largest error arises from the parameters which are extrinsic to the decay  $B \rightarrow X_s + \gamma$  but have crept in due to our procedure of normalizing the branching ratio  $\text{BR}(B \rightarrow X_s + \gamma)$  in terms of the semileptonic branching ratio. To estimate this extrinsic error, we note that the ratio  $m_c/m_b$  can be written as  $m_c/m_b = 1 - (m_b - m_c)/m_b$ . The mass difference  $m_b - m_c$  is known to a very high accuracy through the  $1/m_Q$  expansion [24] or from the semileptonic  $b \rightarrow c$  spectrum; to a rather high accuracy its value is  $m_b - m_c = 3.40$  GeV [25]. The b-quark mass  $m_b$  is, however, not known so precisely. Using for the  $b$  quark pole mass  $m_{b,pole} = 4.8 \pm 0.15$  GeV, one gets  $m_c/m_b = 0.29 \pm 0.02$ , which is consistent with the determination of the same from the lepton energy spectrum  $m_c/m_b = 0.316 \pm 0.013$  [26] but less precise. This introduces considerable uncertainty in the theoretical estimates of the branching ratio  $\text{BR}(B \rightarrow X_s + \gamma)$ , which can be judged from the numerical value  $g(z = 0.29 \pm 0.02) = 0.542 \pm 0.045$ , leading to  $\pm 8.1\%$  error on the branching ratio  $\text{BR}(B \rightarrow X_s + \gamma)$ . We recall here that  $f(z)$  is a slowly varying function of  $z$ , and for the quark mass ratio relevant for the decay  $b \rightarrow c + \ell \nu_\ell$ , namely  $z = 0.29 \pm 0.02$ , it has the value  $f(z) = 2.57 \mp 0.06$ . Taking into account the experimental error of  $\pm 4.1\%$  on  $\text{BR}(B \rightarrow X \ell \nu_\ell)$  [23], and adding these errors linearly, one gets an error of  $\pm 12\%$  on  $\text{BR}(B \rightarrow X_s + \gamma)$  from the semileptonic decays. The procedure that we have adopted in estimating the theoretical uncertainties on the inclusive branching ratio  $\text{BR}(B \rightarrow X_s + \gamma)$  is as follows: We propagate the errors due to the scale  $\mu$ , the QCD scale parameter,  $\Lambda_5$ , and the top quark mass in our calculations. As remarked already, this constitutes the largest error. The extrinsic errors (from  $m_c/m_b$  and the semileptonic branching ratio), being obviously uncorrelated, are then added in quadrature in quoting the branching ratio.

We now proceed to discuss our results. Assuming  $|V_{ts}|/|V_{cb}| = 1$  [22], we plot in Fig. 1 the branching ratio  $\text{BR}(B \rightarrow X_s \gamma)$  as a function of the top quark mass  $m_t$ . For all three solid curves, representing the SM-branching ratio, we have used  $z = 0.29$ . The top solid curve is drawn for  $\mu = 2.5$  GeV and  $\Lambda_5 = 0.260$  GeV. The bottom solid curve is for  $\mu = 10$  GeV and  $\Lambda_5 = 0.145$  GeV, and the middle solid curve corresponds to the central values of the input

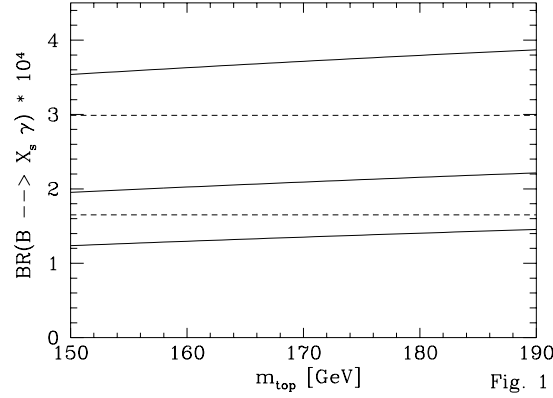


Figure 1:  $\text{BR}(B \rightarrow X_s \gamma)$  as a function of  $m_t$ . The three solid lines correspond to the variation of the parameters  $(\mu, \Lambda_5)$  as described in the text. The experimental  $(\pm 1\sigma)$ -bounds from CLEO [1] are shown by the dashed lines.

parameters in table 2. Using  $\overline{m}_t = (170 \pm 11)$  GeV, and adding the extrinsic error, we get

$$\text{BR}(B \rightarrow X_s + \gamma) = (2.55 \pm 1.28) \times 10^{-4}, \quad (36)$$

to be compared with the CLEO measurement  $\text{BR}(B \rightarrow X_s + \gamma) = (2.32 \pm 0.67) \times 10^{-4}$ . The  $(\pm 1\sigma)$ -upper and -lower bound from the CLEO measurement are shown in Fig. 1 by dashed lines. We see that the agreement between SM and experiment is good. The theoretical errors estimated by us are, however, larger, than for example in [6], for reasons that we have explained above.

In Fig. 2 we show the branching ratio  $\text{BR}(B \rightarrow X_s + \gamma)$  as a function of the CKM matrix element ratio squared  $|V_{ts}|/|V_{cb}|^2$ , varying  $m_t$ ,  $\mu$  and  $\Lambda_5$  in the range specified in table 2. Using

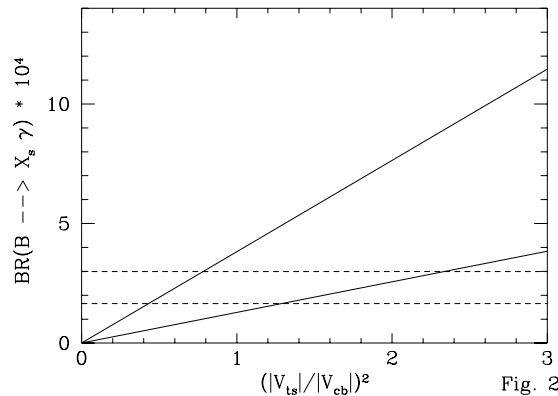


Figure 2:  $\text{BR}(B \rightarrow X_s \gamma)$  as a function of  $(|V_{ts}|/|V_{cb}|)^2$ . The solid lines correspond to the variation of the parameters  $(\mu, \Lambda_5, m_t)$  in the limits specified in table 2. The experimental  $(\pm 1\sigma)$ -bounds from CLEO [1] are shown by the dashed lines.

the  $(\pm 1\sigma)$ -experimental bounds on the branching ratio (dashed lines) we infer

$$|V_{ts}|/|V_{cb}| = 1.10 \pm 0.43, \quad (37)$$

$E_\gamma$ -interval	number of events
1.95 - 2.20 GeV	$229 \pm 256$
2.20 - 2.45 GeV	$484 \pm 163$
2.45 - 2.70 GeV	$381 \pm 105$
2.70 - 2.95 GeV	$12 \pm 59$

Table 3: Photon yield in the laboratory frame from the decay  $B \rightarrow X_s + \gamma$ , obtained from the measurement of the photon energy spectrum by the CLEO collaboration [1] based on a sample of 2.152 million  $B\bar{B}$  events. The data shown have been corrected due to the detector acceptance [27].

which is consistent with the indirect constraints from the CKM unitarity [22].

Now we discuss the photon energy spectrum and fit of the parameters  $p_F$  and  $m_q$  by using the CLEO data which has been corrected for the detector effects. The photon yield from the decay  $B \rightarrow X_s + \gamma$  is given in table 3 in photon energy bins having a width of 250 MeV starting with  $E_\gamma = 1.95$  GeV. We note that these entries are based on the weighted average of the two different methods (event shape and B reconstruction) used by the CLEO collaboration in the analysis of their data [27]. The photon energy has been measured in the laboratory frame (i.e. in the rest frame of  $\Upsilon(4S)$ ) and the numbers in table 3 are presented in this frame. This implies that the  $B$  mesons from the  $\Upsilon(4S)$  decay have a momentum of  $\approx 350$  MeV, and in doing the analysis we have boosted the theoretical rest-frame spectra accordingly. As the theoretical uncertainties are mainly in the normalization of the spectrum, we normalized both the theoretical predictions (parametrized in terms of  $p_F$  and  $m_q$ ) and the experimental data to unit area in the interval between 1.95 GeV and 2.95 GeV. We then performed a  $\chi^2$  analysis. The experimental errors are still large and the fits result in relatively small  $\chi^2$  values; the minimum,  $\chi^2_{min} = 0.038$ , is obtained for  $p_F = 450$  MeV and  $m_q = 0$ , which corresponds to the  $b$ -quark pole mass  $m_{b,pole} = 4.77$  GeV, in good agreement with theoretical estimates of the same. A contour plot in the  $(m_q, p_F)$  plane, obtained by varying the  $\chi^2$  by one unit from  $\chi^2_{min}$ , which corresponds to  $\approx 39\%$  confidence level [22], is shown in Fig. 3. As expected, due to the large errors in data

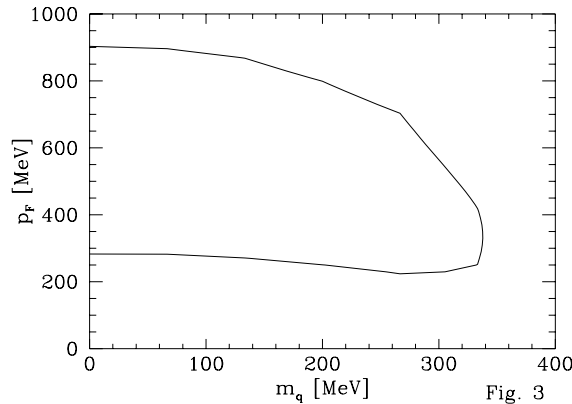


Figure 3: Contourplot in the  $(m_q, p_F)$  parameter space obtained from  $\chi^2 = \chi^2_{min} + 1$ . The minimum  $\chi^2$  is for the values (0 MeV, 450 MeV).

the parameter space cannot be restricted very much at present. Nevertheless, the results for  $p_F$  are compatible with the value  $p_F = 270 \pm 40$  MeV obtained from the  $B$ -semileptonic decay analysis [1]. In Fig. 4 we have plotted the photon energy spectrum normalized to unit area in the interval between 1.95 GeV and 2.95 GeV for the parameters which correspond to the minimum  $\chi^2$  (solid curve) and for another set of parameters that lies near the  $\chi^2$ -boundary in the contour plot (dashed curve). Data from CLEO [1] are also shown.

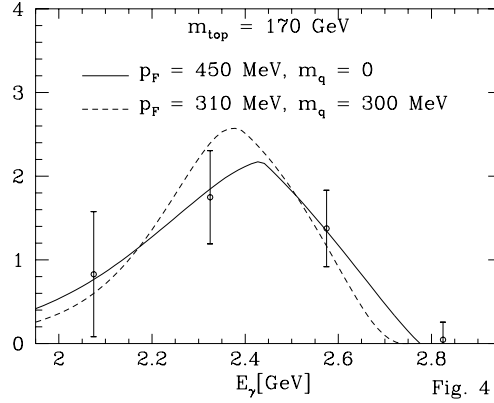


Figure 4: Comparison of the normalized photon energy distribution using the corrected CLEO data [1] and our theoretical distributions, both normalized to unit area in the photon energy interval between 1.95 GeV and 2.95 GeV. The solid curve corresponds to the values with the minimum  $\chi^2$ ,  $(m_q, p_F) = (0, 450 \text{ MeV})$ , and the dashed curve to the values  $(m_q, p_F) = (300 \text{ MeV}, 310 \text{ MeV})$ .

In Fig. 5 we show the comparison of the differential branching ratio from CLEO with our calculations. The theoretical curves correspond to the central values of the input parameters in table 2. The agreement between experiment and SM is good.

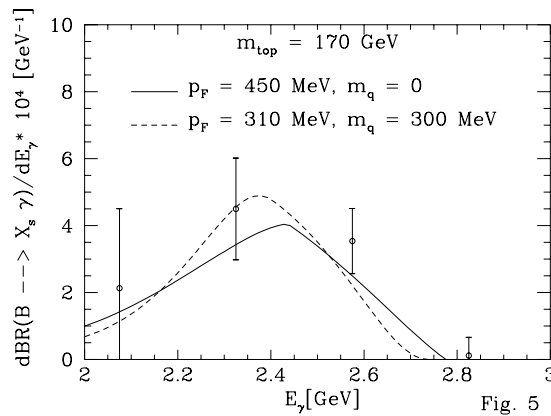


Figure 5: The same as in Fig 4, but with absolute (i.e not normalized) differential branching ratio.

In summary, we have presented an improved theoretical calculation of the branching ratio  $\text{BR}(B \rightarrow X_s + \gamma)$  and the photon energy spectrum in  $B \rightarrow X_s + \gamma$ , using perturbative QCD and

a Gaussian Fermi motion model. We estimate  $\text{BR}(B \rightarrow X_s + \gamma) = (2.55 \pm 1.28) \times 10^{-4}$  in the SM, in agreement with the corresponding branching ratio  $\text{BR}(B \rightarrow X_s + \gamma) = (2.32 \pm 0.67) \times 10^{-4}$  reported by the CLEO collaboration. Our model calculations provide a good account of the measured photon energy distribution, and the best-fit parameters correspond to  $p_F = 450$  MeV and  $m_{b,pole} = 4.77$  GeV. The errors on these parameters are still large but within errors both  $p_F$  and  $m_{b,pole}$  determined from the radiative and semileptonic  $B$  decays are compatible with each other. Precise comparison requires improved measurements and theory, which we hope are forthcoming.

**Acknowledgements** We are very grateful to the members of the CLEO collaboration, in particular Tomasz Skwarnicki and Ed Thorndike, for providing table 3 and for numerous helpful discussions. We acknowledge helpful correspondence and discussions with Matthias Neubert and Vladimir Braun on quark masses. Discussions with Guido Martinelli, Thomas Mannel, Giulia Ricciardi and Daniel Wyler are also thankfully acknowledged. We also thank Frank Cuypers for providing us with a program to draw the contour plot and for useful general discussions on statistics. One of us (C.G.) would like to thank the DESY theory group for its hospitality.

## References

- [1] M.S. Alam et al. (CLEO Collaboration), Phys. Rev. Lett. **74** (1995) 2885.
- [2] R. Ammar et al. (CLEO Collaboration), Phys. Rev. Lett. **71** (1993) 674.
- [3] A. Ali and C. Greub, Z. Phys. **C49** (1991) 431; Phys. Lett. **B259** (1991) 182.
- [4] A. Ali and C. Greub, Phys. Lett. **B287** (1992) 191.
- [5] A. Ali and C. Greub, Z. Phys. **C60** (1993) 433.
- [6] A.J. Buras, M. Misiak, M. Münz, and S. Pokorski, Nucl. Phys. **B424** (1994) 374.
- [7] M. Ciuchini et al., Phys. Lett. **B334** (1994) 137.
- [8] M. Ciuchini et al., Phys. Lett. **B316** (1993) 127; Nucl. Phys. **B415** (1994) 403;  
G. Cella et al., Phys. Lett. **B325** (1994) 227.  
M. Misiak, Nucl. Phys. **B393** (1993) 23; Erratum ibid. **B439** (1995) 461.
- [9] B. Grinstein, R. Springer, and M.B. Wise, Phys. Lett. **202** (1988) 138; Nucl Phys. **B339** (1990) 269.
- [10] A. Ali and E. Pietarinen, Nucl. Phys. **B154** (1979) 519.
- [11] G. Altarelli et al., Nucl. Phys. **B208** (1982) 365.
- [12] T. Inami and C.S. Lim, Prog. Theor. Phys. **65** (1981) 297.
- [13] A. Ali, G. Giudice, and T. Mannel, CERN-TH.7346/94 and Erratum (to appear in Z. Phys. C).
- [14] A. Ali and C. Greub, DESY Report (in preparation).

- [15] G. Corbo, Nucl. Phys. **B212** (1983) 99; N. Cabibbo, G. Corbo, and L. Maiani, *ibid.* **B155** (1979) 93.
- [16] M. Jezabek and J.H. Kühn, Nucl. Phys. **B320** (1989) 20.
- [17] V. Sudakov, Zh. Eksp. Teor. Fiz. **30** (1956) 87 [ Sov. Phys. JETP **3** (1956) 65 ] .
- [18] M. Neubert, Phys. Rev. **D49** (1994) 4623.
- [19] R.D. Dikeman, M. Shifman, and R.G. Uraltsev, Preprint TPI-MINN-95/9-T, UMN-TH-1339-95, UND-HEP-95-BIG05 (hep-ph/9505397).
- [20] J. Chai, H. Georgi, and B. Grinstein, Phys. Lett. **B247** (1990) 399;  
I. Bigi, N. Uraltsev, and A. Vainshtein, Phys. Lett. **B293** (1992) 430; **B297** (1993) 477 (E);  
A. Falk, M. Luke, and M. Savage, Phys. Rev. **D49** (1994) 3367.
- [21] A. Ali, C. Greub and T. Mannel, DESY Report 93-016 (1993), and in *B-Physics Working Group Report, ECFA Workshop on a European B-Meson Factory*, eds.: R. Aleksan and A. Ali, ECFA-Report 93/151, DESY 90-053 (1993).
- [22] L. Montanet et al. (Particle Data Group), Phys. Rev. **D50** (1994) 1173.
- [23] L. Gibbons (CLEO Collaboration), in Proceedings of the XXX Rencontres de Moriond, Les Arcs, March 1994.
- [24] I. Bigi et al., Phys. Rev. Lett. **71** (1993) 496.
- [25] M. Shifman, N.G. Uraltsev, and A. Vainshtein, Phys. Rev. **D51** (1995) 2217;  
M.B. Voloshin, TPI-MINN-94/38-T (hep-ph/9411296).
- [26] R. Rückl, MPI-Ph/36/89.
- [27] E.H. Thorndike and T. Skwarnicki (private communication).